Supplement of Atmos. Chem. Phys. Discuss., 14, 24149–24181, 2014
http://www.atmos-chem-phys-discuss.net/14/24149/2014/
doi:10.5194/acpd-14-24149-2014-supplement

Atmospheric Chemistry and Physics
Discussions
Open Access

Supplement of

Oxidant production from source-oriented particulate matter – Part 1: Oxidative potential using the dithiothreitol (DTT) assay

J. G. Charrier et al.

Correspondence to: C. Anastasio (canastasio@ucdavis.edu)

S1. Soluble metals measurements in DTT solution compared to in surrogate lung fluid

Soluble metals were measured in a surrogate lung fluid (SLF) containing 114 mM NaCl, 2.2 mM KH_2PO_4, 7.8 mM Na_2HPO_4 and anti-oxidants (200 µM ascorbic acid, 300 µM citric acid, 100 µM glutathione and 100 µM uric acid), pH of 7.4. Portions of filters were extracted from 1.5 to 24 hours at room temperature on a shake table. DTT assay conditions are somewhat different: the extraction fluid contains 22 mM KH_2PO_4, 78 mM Na_2HPO_4 and 100 µM DTT, pH 7.4, and is extracted for 20 minutes at 37 ˚C. Both the SLF and DTT extraction solutions were treated with Chelex 100 resin to remove transition metals prior to adding the antioxidants or DTT. The differences in ligands, extraction time and temperature for the two assays could affect soluble metals measurements. To test this, we measured soluble metals under the DTT assay conditions for 12 of the 38 samples (6 summer and 6 winter, 7 SMF and 5 UF). The resulting soluble metal concentrations were very similar for the SLF and DTT extractions, with the exception of (Fig. S1). Fe was sometimes higher in the SLF than the DTT assay, possibly because of the presence of citrate in the SLF, which effectively solubilizes Fe (Aust et al., 2002). Given the similarity in the metals data for the two assays, we use the SLF measurements since these were made for every sample as part of our companion study (Richards-Henderson et al., 2014). The SLF results might sometimes overestimate Fe in the DTT extracts, but this is a minor issue since Fe is nearly always unimportant in the DTT assay (Charrier and Anastasio, 2012).

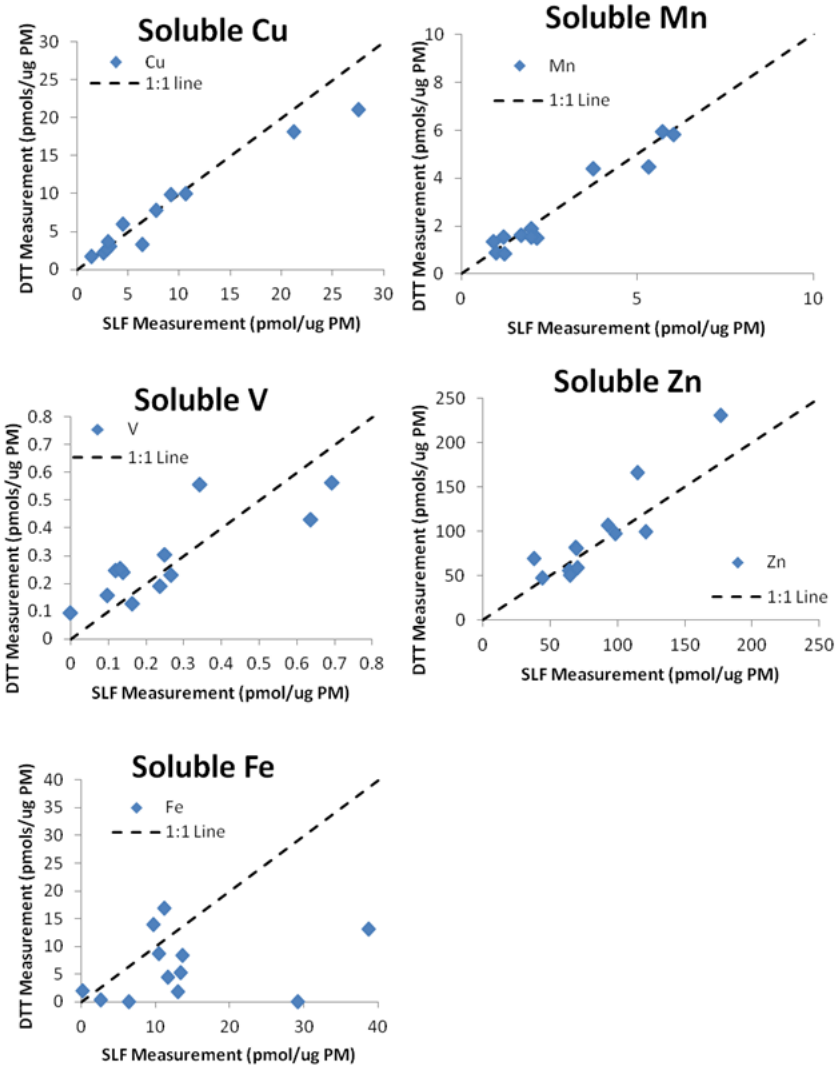

Figure S1. Comparison of soluble metals measurements in DTT solution versus SLF solution.

S2. Total and soluble metals

To measure total metals, approximately 167 µg of extracted PM from each source was digested using 1 M nitric acid via sonication and diluted to 6 mL for sample analysis. All samples were analyzed in triplicate for a standard set of 26 elements. A description of soluble metals analysis steps is in Section 2.5 of the main text.

Both total and soluble metals were analyzed by the Interdisciplinary Center for Plasma Mass Spectrometry at the University of California at Davis (ICPMS.UCDavis.edu) using an Agilent 7500CE ICP-MS (Agilent Technologies, Palo Alto, CA). The prepared samples were introduced using a MicroMist Nebulizer (Glass Expansion) into a temperature controlled spray chamber with He as the collision cell gas. Instrument standards were diluted from Certiprep ME2A standard (SPEX CertiPrep) to 0.25ppb, 0.5ppb, 1ppb, 10ppb, 100ppb, 200ppb and 500ppb respectively in 3% Trace Element HNO$_3$ in ultrapure water. A NIST 1643E Standard was analyzed initially and QC standard consisting of ME2A at 100ppb were analyzed every 12th sample as quality controls. An internal standard consisting of Sc, Y, and Bi Certiprep standards (SPEX CertiPrep) were diluted to 100ppb in 3% HNO3 and introduced by peripump. Soluble metals results are in the main text Fig. 1, while total metals results are in Fig. S2 below.

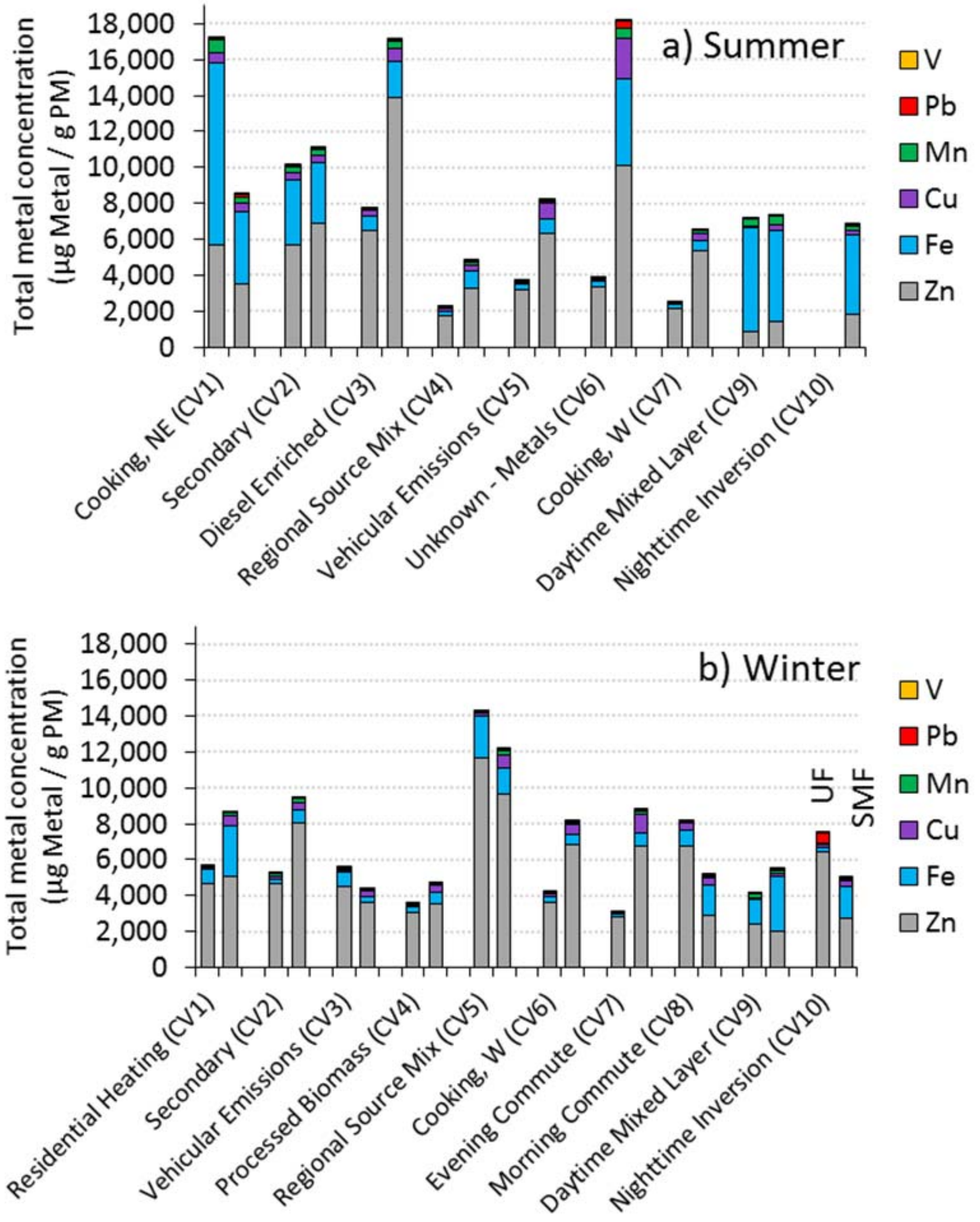

Figure S2. Total metals concentration in each sample. For each CV, the first bar is the UF size fraction and the second bar is the SMF size fraction. Zn concentrations are divided by 10. In panel (a) there is no data for the CV 10 UF sample.

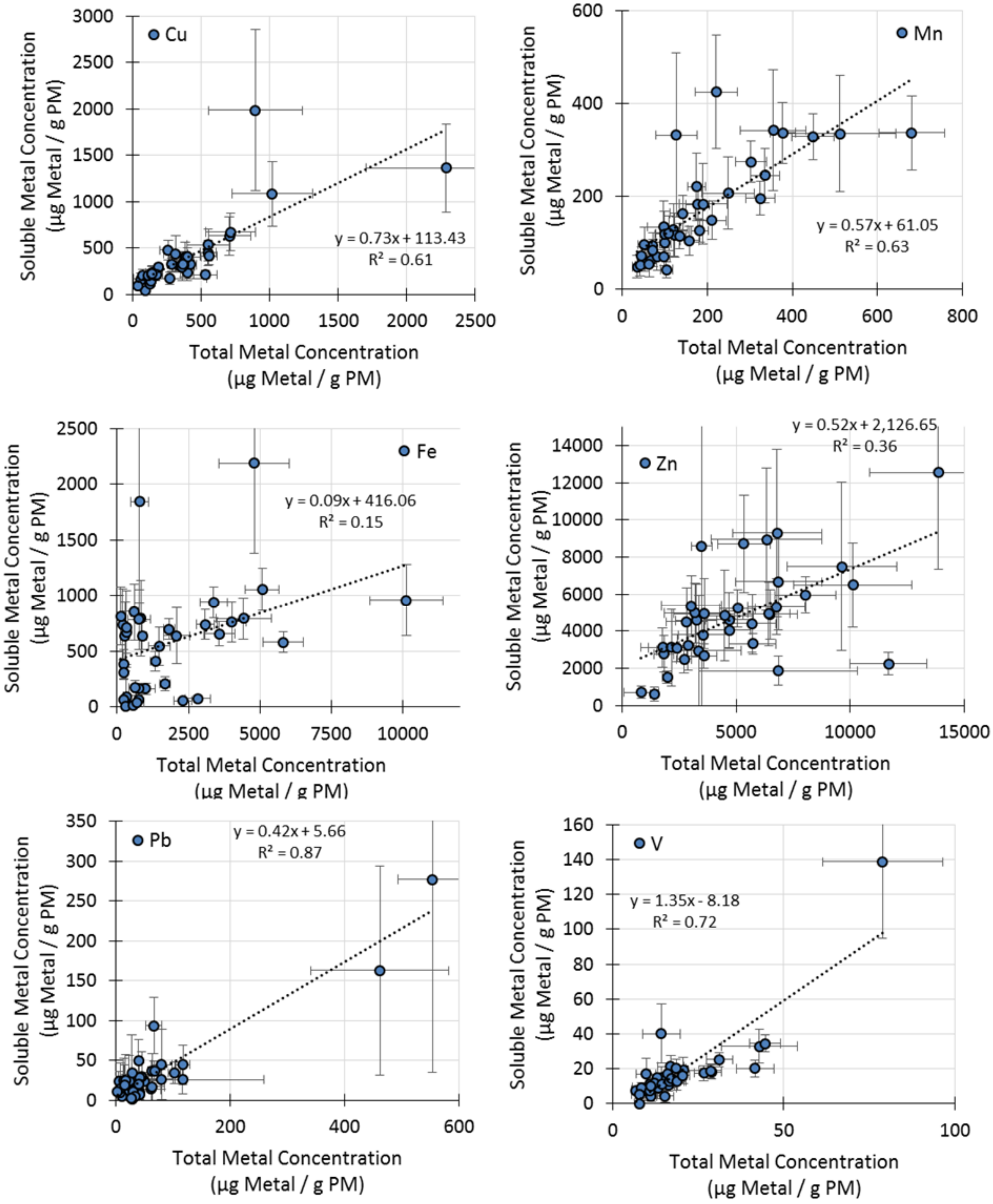

Figure S3. Correlations between total and soluble metals data.

Table S1. Range of atmospheric concentrations of total and soluble metals for each season and size fraction

Metal	Total Metals Median and Range of Concentration (ng/m^3)			
	Summer 2008		Winter 2009	
	UF	SMF	UF	SMF
Zn	12 (1.9-20)	29 (8.8-128)	19 (4.7-60)	31 (4.7-79)
Ba	4.4 (1.3-11)	4.0 (0.89-7.8)	8.9 (1.1-34)	1.6 (0.30-4.9)
Fe	1.8 (0.40-31)	31 (3.1-44)	2.6 (0.30-12)	6.1 (2.7-24)
Cu	0.44 (0.15-1.7)	4.3 (1.9-21)	0.68 (0.092-1.2)	3.5 (0.42-6.3)
Mn	0.32 (0.084-2.1)	2.3 (0.72-4.7)	0.42 (0.10-0.63)	0.72 (0.30-1.9)
Ni	0.13 (0.091-0.44)	0.80 (0.50-2.5)	0.27 (0.033-1.0)	0.65 (0.21-2.0)
Pb	0.079 (0.013-0.31)	0.56 (0.20-4.2)	0.092 (0.005-1.1)	0.25 (0.12-0.51)
V	0.044 (0.02-0.13)	0.24 (0.087-0.61)	0.051 (0.018-0.11)	0.07 (0.032-0.16)
Cr	0.056 (0.018-0.26)	0.66 (0.24-10)	0.13 (0-0.29)	0.25 (0.14-0.82)
Cd	0.01 (0.005-0.022)	0.05 (0.035-0.17)	0.03 (0.004-0.098)	0.044 (0.013-0.39)
Co	0.009 (0.004-0.041)	0.055 (0.027-0.16)	0.017 (0.002-0.025)	0.032 (0.014-0.12)
Metal	Soluble Metals Median and Range of Concentration (ng/m3)			
	Summer 2008		Winter 2009	
	UF	SMF	UF	SMF
Zn	10 (1.6-18)	44 (3.8-116)	15 (6.0-44)	35 (3.6-77)
Ba	3.7 (0.70-5.3)	2.8 (0.36-8.2)	4.6 (0.63-14)	0.78 (0.19-3.3)
Fe	2.0 (0.34-2.9)	6.2 (1.5-20)	1.0 (0.053-5.9)	1.5 (0.16-5.6)
Cu	0.65 (0.11-1.3)	3.7 (1.6-15)	0.79 (0.21-2.0)	3.0 (0.51-6.2)
Mn	0.47 (0.10-1.0)	2.3 (0.83-3.3)	0.42 (0.12-0.79)	0.74 (0.28-1.6)
Ni	0.16 (0.057-0.87)	0.61 (0.16-1.5)	0.28 (0.086-2.6)	0.12 (0-5.0)
Pb	0.058 (0.016-0.10)	0.31 (0.05-1.)	0.14 (0.024-0.53)	0.077 (0.01-0.17)
V	0.039 (0.025-0.16)	0.21 (0.11-1.1)	0.028 (0-0.074)	0.066 (0.036-0.18)
Cr	0.084 (0.034-0.73)	0.34 (0.098-0.56)	0.12 (0.029-0.40)	0.074 (0-0.35)
Cd	0.005 (0-0.50)	0.068 (0-1.2)	0.052 (0-5.6)	0.028 (0-0.32)
Co	0.007 (0.004-0.065)	0.046 (0.022-0.085)	0.021 (0.002-0.34)	0.017 (0.004-0.098)

Note: Co, Cr, Cd and Ni were generally below their detection limits.

S3. Percent solubility

We calculated the percent of each metal that was soluble in SLF for each CV and size range as the ratio between the SLF-soluble concentration and the total metal (acid-extract) concentration. Figure S3 shows the percent solubility for the 6 metals that are well measured: V, Mn, Cu, Fe, Zn, Pb. Four metals were generally below detection: Co, Cr, Cd. Total metals data for summer ultrafine “Nighttime Inversion (CV10)” is missing, so percent solubility for that CV cannot be calculated. V, Mn, Cu and Zn all exhibited nearly 100% solubility. Pb is less soluble, with a median solubility of 48% and Fe was generally the least soluble metal measured, with a median solubility of 27%.

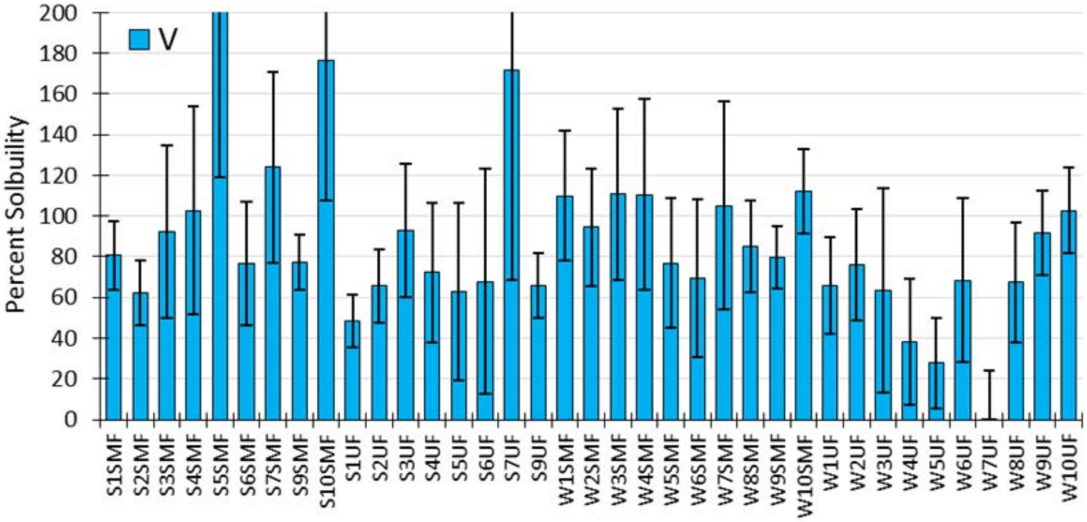
V
Percent Solbuility
0
20
40
60
80
100
120
140
160
180
200
S1SMF
S2SMF
S3SMF
S4SMF
S5SMF
S6SMF
S7SMF
S9SMF
S10SMF
S1UF
S2UF
S3UF
S4UF
S5UF
S6UF
S7UF
S9UF
W1SMF
W2SMF
W3SMF
W4SMF
W5SMF
W6SMF
W7SMF
W8SMF
W9SMF
W10SMF
W1UF
W2UF
W3UF
W4UF
W5UF
W6UF
W7UF
W8UF
W9UF
W10UF

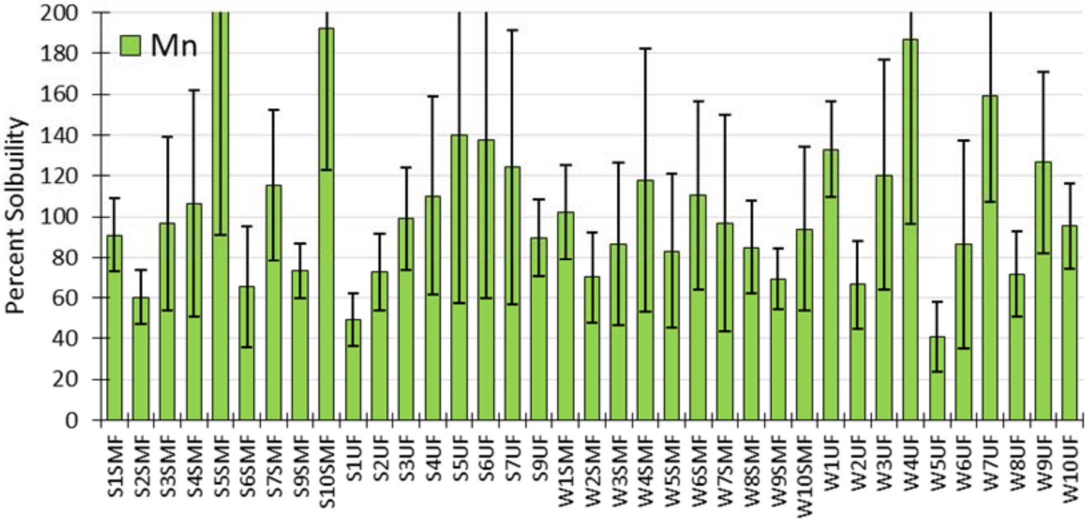
Mn
Percent Solbuility
0
20
40
60
80
100
120
140
160
180
200
S1SMF
S2SMF
S3SMF
S4SMF
S5SMF
S6SMF
S7SMF
S9SMF
S10SMF
S1UF
S2UF
S3UF
S4UF
S5UF
S6UF
S7UF
S9UF
W1SMF
W2SMF
W3SMF
W4SMF
W5SMF
W6SMF
W7SMF
W8SMF
W9SMF
W10SMF
W1UF
W2UF
W3UF
W4UF
W5UF
W6UF
W7UF
W8UF
W9UF
W10UF

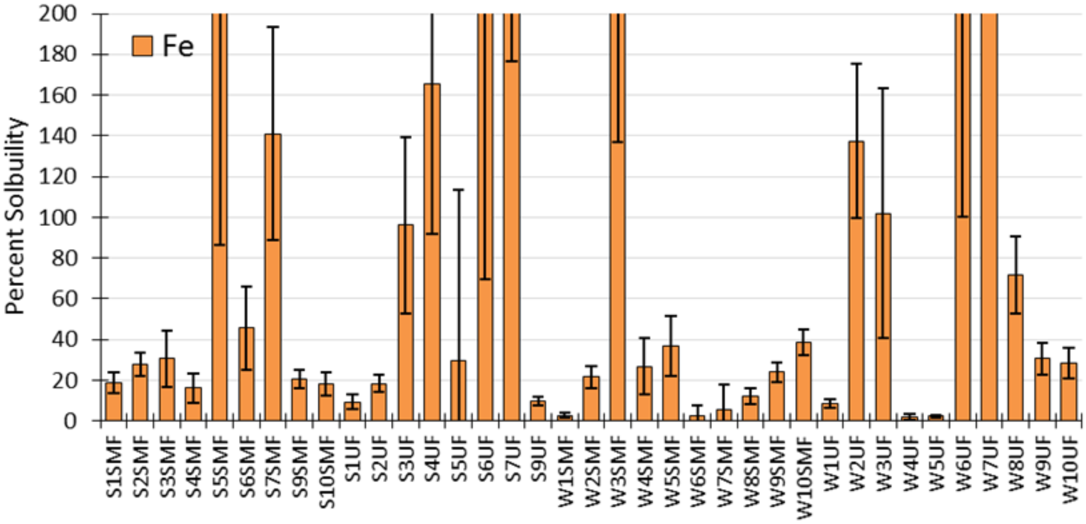
Fe
Percent Solbuility
0
20
40
60
80
100
120
140
160
180
200
S1SMF
S2SMF
S3SMF
S4SMF
S5SMF
S6SMF
S7SMF
S9SMF
S10SMF
S1UF
S2UF
S3UF
S4UF
S5UF
S6UF
S7UF
S9UF
W1SMF
W2SMF
W3SMF
W4SMF
W5SMF
W6SMF
W7SMF
W8SMF
W9SMF
W10SMF
W1UF
W2UF
W3UF
W4UF
W5UF
W6UF
W7UF
W8UF
W9UF
W10UF

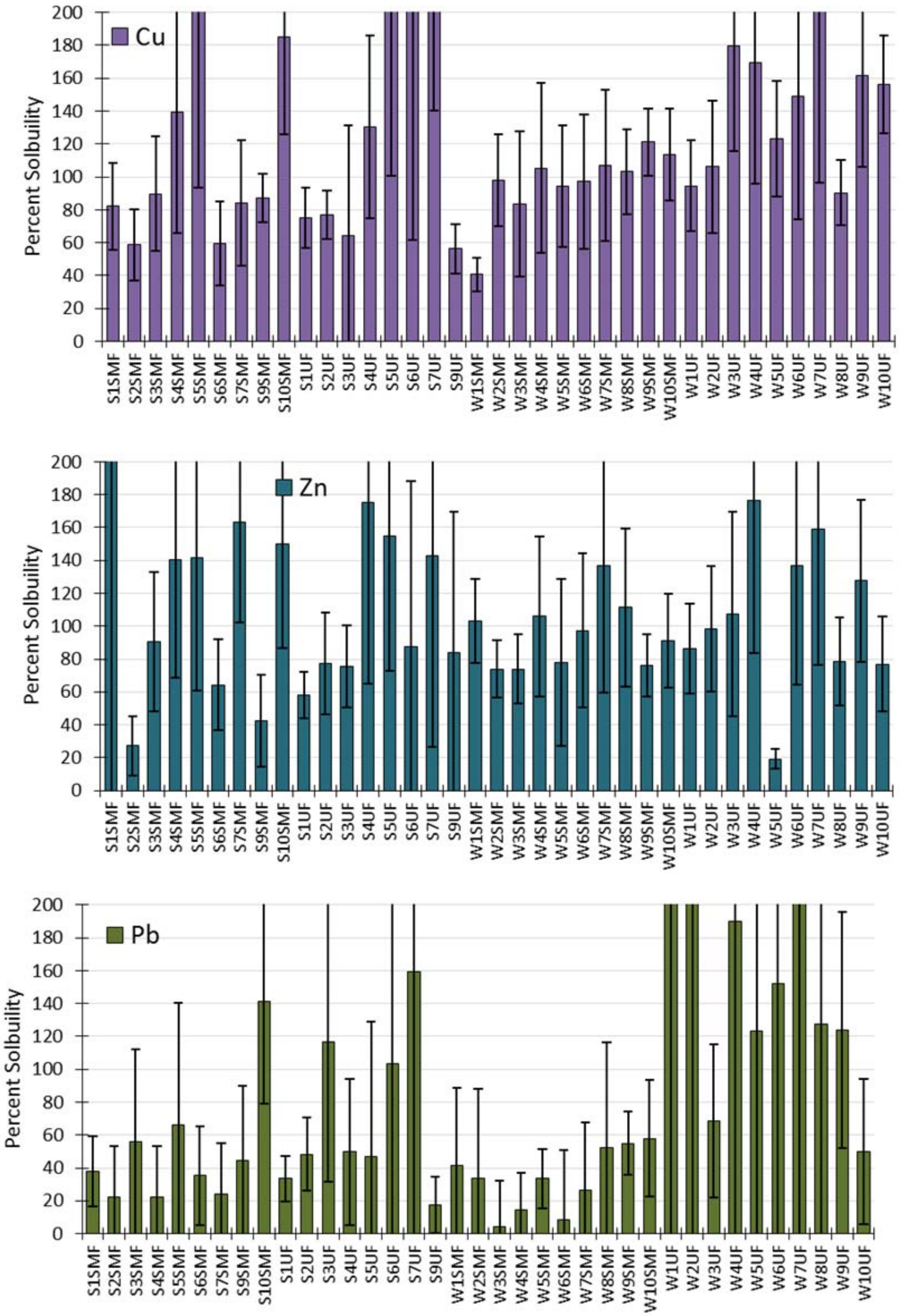

Figure S4. Percent solubility for each metals and CV. Error bars are the propagated errors of soluble and total metals data accounting for both blank corrections and error in the mass data.

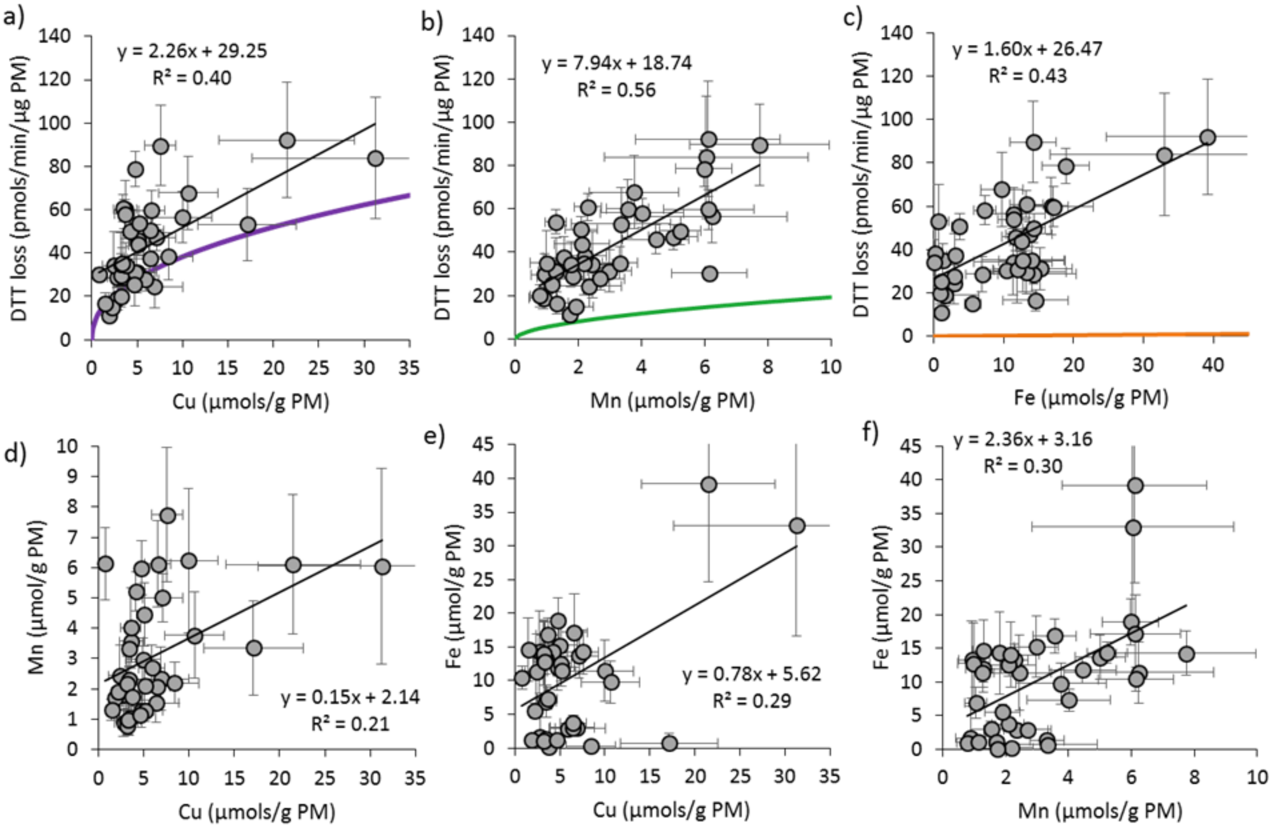

Figure S5. Correlations of DTT loss with soluble Cu, Mn, and V (a – c) and correlations between these soluble metal concentrations (d – f). The lines in a – c represent the calculated DTT response as a function of metal concentration for 30 µg of PM based on the concentration-response curves in Charrier and Anastasio (2012).

Table S2. PM masses used for DTT analysis (sample volume is 3.0 mL).

Experiment	**ChemVol**	UF		SMF	
		Mass (µg)	Error	Mass (µg)	Error
Summer 2008 Samples	1	38.2	3.8	38.2	3.8
	2	38.2	3.8	38.2	3.8
	3	29.4	3.7	28.0	5.6
	4	31.4	7.8	36.1	9.0
	5	24.7	6.2	18.7	6.2
	6	18.0	6.0	17.6	4.4
	7	17.6	4.4	31.4	6.3
	9	9	0.3	32.3	3.2
	10	56.8	N/A	18.2	3.6
Winter 2009 Samples	1	37.3	3.9	29.4	4.2
	2	29.4	3.9	29.4	4.2
	3	31.4	6.7	29.4	4.2
	4	24.7	6.7	31.4	7.8
	5	31.4	3.9	28	7.0
	6	30	7.5	28	7.0
	7	29.4	4.5	20.0	5.0
	8	32.3	3.3	32.3	3.2
	9	39.0	4.4	32.3	3.2
	10	8	0.6	31.0	3.1
Field Blanks		2.0	--	2.0	--

S4. Estimating the contribution of PQN to DTT response

To test if PQN is likely important in our samples we assume ambient particulate PQN was present at the median measured concentration previously reported (0.3 ng/m^3) (Charrier and Anastasio, 2012). Using the mass concentration of each sample (Table 1 in the main text) and the mass of PM added to each vial (Table S2), we calculated the expected concentration of PQN in each solution. We then used the PQN concentration-response equation from Charrier and Anastasio (2012) to calculate the DTT response from PQN in each DTT extract and calculated what percent of the DTT response this would contribute to each sample. Results are discussed in the main text.

S5. Apportionment of volume-normalized oxidative potential to individual sources.

We categorized the sources we observed and those in the modeling of Hu et al. (2014) into four categories: Cooking, Mobile, Heating, Biomass/Wood Smoke. Any sources that do not fit these categories are labeled “Other”. The sources included in each category are listed in Supplemental Tables S3 and S4. We calculated the average ambient mass concentration for each category over our two-week sampling periods using the 7-year average source contributions from 2000 – 2006 provided in Hu et al.

(2014). We multiplied the mass concentration of each category by the weighted average of the mass-normalized oxidative potential (Fig. 2) for the associated category to get the volume-normalized oxidative potential of each category. We then summed the volume-normalized oxidative potential of each category (Fig. 4c and 4d). There is a remaining volume-normalized oxidative potential measured from the PM which is not accounted for by the four source categories. We attribute this to “Unknown” sources, which includes the “Other” category, sources that were not identified in the emissions inventory, and secondary PM mass, which is not accounted for in the primary modeling data of Hu et al. A large percent of PM mass is identified in “Other”, which consists of constrained and unconstrained PM sources (Fig. S6).

Our approach makes several assumptions. First, our measurements are for $PM_{1.0\text{-}0.17}$ and $PM_{0.17}$, while corresponding model results are for $PM_{2.5}$ and $PM_{0.1}$, respectively. Secondly, our samples were collected in 2008 and 2009 while model sources are from 2000 – 2006. And finally, model sources only account for primary PM mass, so contribution from secondary PM mass is automatically grouped into “Unknown”. Though these assumptions are not ideal, the data from Hu et al. (2014) are the most complete estimates of PM sources in Fresno currently available, especially in regards to the ultrafine size fraction.

Table S3. ARB emissions inventory PM sources from (Hu et al., 2014) with their associated category.

Source	Category
Agricultural pruning waste burning	Biomass/Wood Smoke
Agricultural crop waste burning	Biomass/Wood Smoke
Residential wood stoves	Biomass/Wood Smoke
Residential wood fireplaces	Biomass/Wood Smoke
Non-agricultural waste burning	Biomass/Wood Smoke
Commercial deep fat frying	Cooking
Commercial cooking unspecified	Cooking
Commercial Charbroiling	Cooking
Industrial residual oil combustion	Heating
Residential natural gas water heating	Heating
Residential natural gas space heating	Heating
Offroad trans refrigeration diesel	Mobile
offroad industrial diesel equipment	Mobile
Ag. Irrigation diesel engines	Mobile
Light commercial gasoline equipment	Mobile
Light commercial diesel equipment	Mobile
Lawn and garden gasoline 2-st	Mobile
Onroad diesel exhaust	Mobile
lawn and garden diesel equipment	Mobile
Construction and mining diesel	Mobile
Industrial gasoline equipment 4-st	Mobile
Lawn and garden gasoline 4-st	Mobile
Onroad non-cat. gasoline hot exhaust	Mobile
Trains hauling locomotives	Mobile
Stationary IC diesel engines	Mobile
Agricultural diesel equipment	Mobile
Recreational gasoline boat (unspec) 2-st	Mobile
Onroad cat. gasoline hot exhaust	Mobile
Cat. gasoline buses	Mobile
Onroad cat. gasoline cold exhaust	Mobile
Onroad diesel idle	Mobile
Non-cat. gasoline cold exhaust	Mobile
Onroad diesel buses	Mobile
Construction and mining gasoline	Mobile
Paved road dust freeways	Mobile
Paved road dust local streets	Mobile
Paved road dust major streets	Mobile
Commercial natural gas combustion	Other
Commercial LPG combustion	Other
Ag. land windblown dust	Other
Commercial bldg construction&demolition	Other
Farming tilling dust	Other
Industrial bldg construction&demolition	Other
Institutional bldg construction&demolition	Other
Non-constrained PM2.5 sources	Other
Unpaved road dust farm roads	Other
Oil drill diesel equipment	Other
Other constrained PM0.1 sources	Other
Other constrained PM2.5 sources	Other
Residential bldg construction&demolition	Other
Stationary IC diesel engines	Other
Structural fires	Other
Non-constrained PM0.1 sources	Other

Table S4. Sources identified during our sampling with associated categories.

CV	Source	Category
Summer		
1	Cooking - NE	Cooking
7	Cooking - W	Cooking
3	Diesel enriched	Mobile
5	Vehicular emissions	Mobile
2	Secondary	Other
4	Regional source mix	Other
6	Unknown - metals	Other
10	Nighttime Inversion	Other
9	Daytime mixed layer	Other
Winter		
4	Processed biomass	Biomass
6	Cooking - W	Cooking
1	Residential heating	Heating
3	Vehicular emissions	Mobile
8	Morning commute	Mobile
2	Secondary	Other
5	Regional source mix	Other
10	Nighttime inversion	Other
9	Daytime mixed layer	Other
7	Evening commute	Other

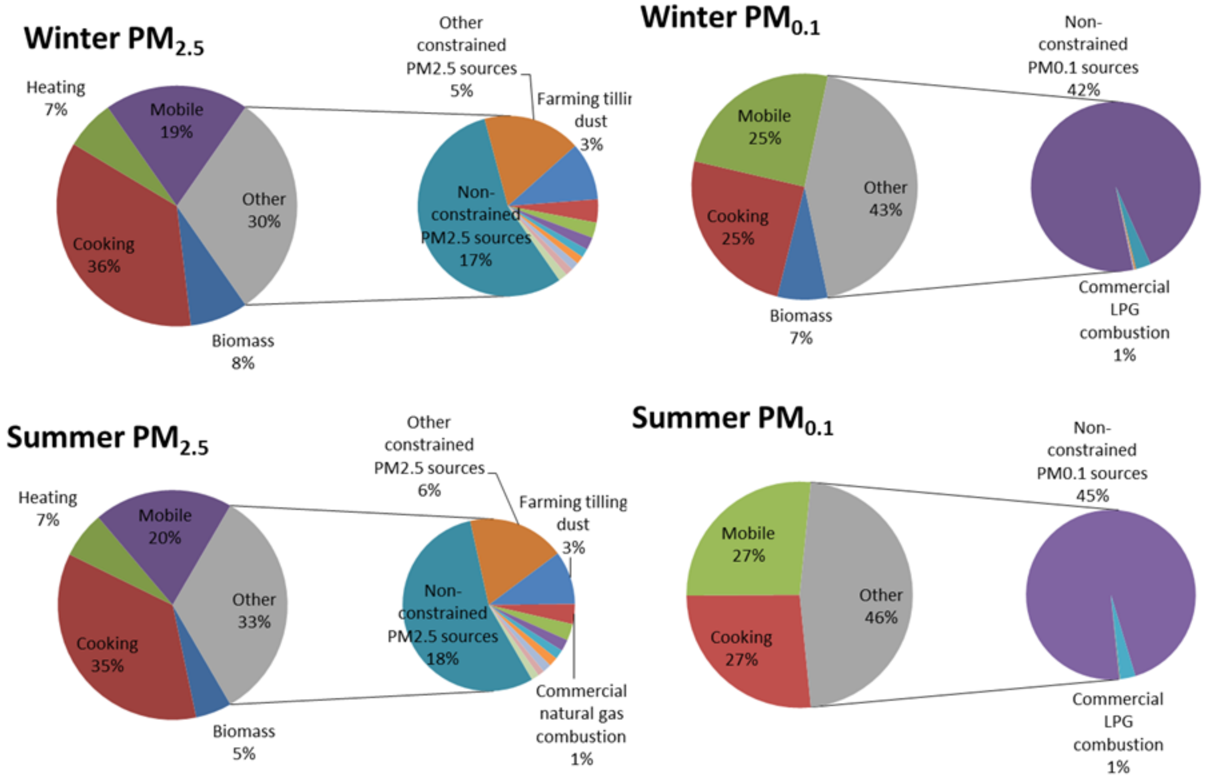

Figure S6. Contribution of source categories to total primary PM mass in Fresno, CA as identified by modeling for the time period that match ambient samples (Hu et al., 2014). To match previous nomenclature, “winter” is actually 3/1/2009 to 4/6/2009 and “summer” is actually 9/11/2008 to 10/21/2008 is designated “summer” (see main text methods discussion). A detailed summary of sources contributing to the “Other” category is shown in each expansion pie charts.

References

Aust, A. E., Ball, J. C., Hu, A. A., Lighty, J. S., Smith, K. R., Straccia, A. M., Veranth, J. M., and Young, W. C.: Particle characteristics responsible for effects on human lung epithelial cells, Research Report/Health Effects Institute, 1-65; discussion 67-76, 2002.

Charrier, J. G., and Anastasio, C.: On dithiothreitol (DTT) as a measure of oxidative potential for ambient particles: evidence for the importance of soluble transition metals., Atmos. Chem. Phys., 12, 9321-9333, 2012.

Hu, J., Hongliang, Z., Chen, S., Ying, Q., Wiedinmyer, C., Vandenberghe, F., and Kleeman, M.: Identifying $PM_{2.5}$ and $PM_{0.1}$ sources for epidemiological studies in California, Env. Sci. Technol., 48, 4980-4990, 2014.

Richards-Henderson, N. K., Charrier, J. G., Bein, K. J., Bau, D., Wexler, A. S., and Anastasio, C.: Oxidant production from source-oriented particulate matter – Part 2: Hydrogen peroxide and hydroxyl radical, Atmos. Chem. Phys., Submitted, 2014.